Elastic Scattering of One Neutron Halo Nuclei

Awad A. Ibraheem [(a)] *,M. A. Hassanin [(b)]†And M. El-Azab Farid[(c)] ‡

[(a)] Faculty of Science, Al-Azhar University (Assuit) 71524, Egypt.

[(b)] Faculty of Education, Assuit University, El-Kharga, New-Valley, Egypt.

[(c)] Physics Department, Assiut University, Assiut 71516, Egypt.

Abstract

The double folding optical potential of the ^{11}Be+^{208}Pb reaction has been constructed using the JLM effective interaction. The total reaction cross sections and the elastic scattering differential cross sections at E =20 - 80 MeV/nucleon have been obtained using the derived potentials with and without including the breakup potentials .

PACS number(s): 25.60.-t,24.10.Ht,27.20.+n,25.60.Bx

Keywords: Optical model, Elastic scattering, Halo nuclei, Folding model

*awad_ah_eb@yahoo.com

†mho1959@yahoo.com

‡faridme71516@yahoo.com

1 Introduction

Recent experiments with radioactive nuclear beams [1] have revealed in the last two decades a new phenomenon called ***"nuclear halo"***. This phenomenon was first observed in the mid-eighties during the determination of the reaction cross sections for the interaction of neutron-rich nuclei with various targets at high energies [2]. At that time, the unusually significant increase in the reaction cross sections observed for neutron-rich nuclei is an indication for the unexpected increase in the nuclear radius.

Therefore, it has been established from the study of the structural properties of neutron-rich isotopes of lightest elements that nuclei such as ^{6,8}He, ^{11}Li, ^{11,12,14}Be,^{17}B and ^{16,19}C have a localized central core surrounded by a dilute halo of neutrons.

The angular distributions of elastic and inelastic scattering of neutron-rich nuclei on proton, carbon , silicon and lead targets at intermediate energies are studied in several articles [3, 4]. It has been established that halo breakup is responsible for a damping in the elastic scattering angular distribution in the range $\sim 5^0 - 20^0$. Also from studying charge exchange reactions it was found that the halo breakup effect reduces the absolute cross sections by about 50% [5]. Thus, one must take into account the couplings to transitions to the low-lying excited states as well as to the resonance and breakup (continuum) states. This means that the bare nucleus-nucleus optical potential should be supplemented by the so called dynamic polarization potential (DPP). Contributions from the DPP to the optical potential may be simulated by a surface phenomenological correction using splines added to the real part of the potential [6] or using a complex phenomenological surface Woods-Saxon (WS) potential with a repulsive real part [7].

Recently, in our previous paper[8] we studied the core recoil and nuclear breakup of the valence nucleon. A microscopic absorptive potential is obtained within a semiclassical approach and the angular distribution of the elastic scattering cross sections of ^{11}Be+^{208}Pb at 20-80 MeV/nucleon were calculated using a Woods-Saxon potentials plus the DPP which comes from the calculated Coulomb and nuclear breakup effects. It would much more satisfactory if the full potential could be derived from a microscopic basis so that there would be no free parameters at all in the model. In the present work we test the double folding (DF) approach based on what is the so- called Jeukenne, Lejeune and Mahaux (JLM) interaction [9] to reanalyze the ^{11}Be+^{208}Pb at 20-80 MeV/nucleon with full microscopical potentials with and without including DPP. The derived reaction cross sections are investigated. The effects of changing the form of the nuclear density of ^{11}Be nucleus on the results is considered.

2 Formalism

The optical model potential is an effective interaction V(R) between the two, projectile and target, nuclei separated by the distance R, which can be used in the conventional non relativistic Schrdinger

equation

$$[-\frac{\hbar^2}{2\mu}\nabla^2 + V(R) - E_{CM}]\chi(R) = 0 \tag{1}$$

The asymptotic behavior of its solutions $\chi(R)$ describes the projectile target elastic scattering when the projectile and target are well separated,μ is the reduced mass of the system and E_{CM} is the energy of the relative motion in the center-of-mass system. The potential V(R) can be expressed as

$$V(R) = V_C(R) - U(R, E) \tag{2}$$

where the Coulomb potential $V_C(R)$ represents the interaction of the charge of the incident projectile, $Z_P e$, with the charge distribution due to protons, $Z_T e$ in the target nucleus which is usually considered as a homogeneously charged sphere of radius R_C. Then we get

$$V_C(R) = \frac{Z_p Z_t e^2}{2R_C}(3. - \frac{R^2}{R_C^2}), R \leq R_C \tag{3}$$

and

$$V_C(R) = \frac{Z_p Z_t e^2}{R}, R \geq R_C \tag{4}$$

where the Coulomb radius $R_C = r_C(A_P^{1/3} + A_T^{1/3})$ and r_C is the radius parameter. The central optical potential $U(R, E)$ is complex . The nucleus nucleus real $V^{DF}(R, E)$ and imaginary volume $W_v^{DF}(r, E)$ potentials are expressed as:-

$$V^{DF}(R, E) = \int\int \rho_{^{11}Be}(r_1)\rho_{^{208}Pb}(r_2) \times \upsilon_{nn}(s, \rho_{^{11}Be}, \rho_{^{208}Pb}, E)d\overrightarrow{r_1}d\overrightarrow{r_2} \tag{5}$$

where , $s = |\bar{R} - \bar{r}_1 + \bar{r}_2|$ and

$$W_v^{DF}(r, E) = \int\int \rho_{^{11}Be}(r_1)\rho_{^{208}Pb}(r_2) \times \omega_{nn}(s, \rho_{^{11}Be}, \rho_{^{208}Pb}, E)d\overrightarrow{r_1}d\overrightarrow{r_2} \tag{6}$$

where ρ denotes for the nuclear density and υ_{nn} and ω_{nn} for the real and imaginary part of the effective nucleon nucleon (NN) interaction.

While, according to [10] the surface imaginary optical potential $W_S(\mathbf{R}(t), E)$ due to breakup can be related to the breakup probability as

$$\int_{-\infty}^{+\infty} W_S(\mathbf{R}(t), E)dt = -\frac{\hbar}{2}P_{b_{up}}(b_c) \tag{7}$$

where $P_{b_{up}}$ are the breakup probabilities in the various channels. The total breakup probability will be given by the nuclear $p_{b_{up}}^N(b_c)$ and Coulomb breakup $p_{b_{up}}^C(b_c)$ as

$$p_{b_{up}}(b_c) = P_0(b_c)(p_{b_u p}^N(b_c) + p_{b_{up}}^C(b_c)). \tag{8}$$

and $R(t) = b_c + \nu t$ is the classical trajectory of relative motion for the nucleus nucleus collision. The core survival probability has been parameterized as [11]

$$P_0(r) = |S_{CT}|^2 = \exp(-\ln 2e^{[(R_s - r)/a_0]}), \tag{9}$$

with the strong absorption $R_s = 1.4(A_P^{1/3} + A_T^{1/3})fm$ and $a_0 = 0.6fm$ [11, 12]. And, S_{CT} is the scattering s-matrix due to the core-target interaction.

The effective interaction of (JLM)[9] is obtained in a Brueckner-Hartree-Fock (BHF) approximation from the Reid soft-core NN potential. This interaction is complex, energy and density-dependent and, therefore, provides simultaneously both real and imaginary volume parts of the DF optical potential.

The real and imaginary parts of the JLM effective interaction are expressed respectively as[9, 13]

$$\upsilon_{nn}(s, \rho_{^{11}Be}, \rho_{^{208}Pb}, E) = (1 - \beta_R \rho_{^{11}Be}^{2/3})\nu_1(\rho_{^{208}Pb}, E)h(s)$$
$$\omega_{nn}(s, \rho_{^{11}Be}, \rho_{^{208}Pb}, E) = (1 - \beta_R \rho_{^{11}Be}^{2/3})\nu_2(\rho_{^{208}Pb}, E)h(s) \quad (10)$$

where, β_R and β_I are the projectile density dependence parameters for the real and imaginary parts respectively, and

$$h(s) = \frac{1}{(t\sqrt{\pi})^3} \exp(-s^2/t^2). \quad (11)$$

The range parameter t is chosen to equal 1.2 fm for both real and imaginary parts. Derivation details of $\nu_1(\rho_{^{208}Pb}, E)$ and $\nu_2(\rho_{^{208}Pb}, E)$ components are shown in Refs.[9, 13].

The real and imaginary DF potentials (5,6)are obtained using the modified momentum space folding code DFPOT[14, 15]. As already discussed in Refs.[8, 16], the imaginary surface potentials proposed to account for the nuclear and Coulomb are respectively given by :-

$$W_S^N(R, E) = -\frac{\hbar v}{2} p_{bup}^N(R) \frac{1}{\sqrt{2\pi\alpha_n R}} \quad (12)$$

and

$$W_S^C(R, E) = -\frac{\hbar v}{2} p_{bup}^C(R) \frac{1}{\sqrt{2\pi\beta_n R}} \quad (13)$$

with,

$$p_{bub}^N(R) = \sum_n A_n \ \exp(-R/\alpha_n), \quad (14)$$

$$p_{bub}^C(R) = \sum_n B_n \ \exp(-R/\beta_n), \quad (15)$$

The dimensionless coefficients A_n and B_n and range parameters α_n and β_n in (fm)are given found in Table 2 of Ref.[8].

2.1 Nuclear matter densities

Several studies [17, 18] have generally assumed the neutron halo nuclei to be composed of a compact nuclear core surrounded by a halo of neutron(s). Following this prescription, we consider the 1n-halo nucleus ^{11}Be to be composed of a ^{10}Be core and a halo of one neutron. Hence, we propose the density of ^{11}Be nucleus as:

$$\rho_{^{11}Be}(r) = \rho_{^{10}Be}(r) + \rho_n(r) \quad (16)$$

It is well known ^{11}Be nucleus contains an intruder $2s_{1/2}$ neutron configuration in its ground state, although the $1p_{1/2}$ configuration is normally expected. The energy of the $2s_{1/2}$ becomes very low because of the large asymmetry in the proton and neutron numbers.

The density distribution of ^{10}Be core is assumed to be of a Fermi form as [19]

$$\rho_{^{10}Be}(r) = \rho_0/[1 + exp(\frac{r - 2.0}{0.511})] \tag{17}$$

where ρ_0 can be determined from the normalization condition

$$4\pi \int \rho(r) r^2 dr = 10 \tag{18}$$

This density produces a root mean square (rms) radius, $\langle r^2_{rms} \rangle^{1/2}$ of ^{10}Be nucleus equals 2.45 fm. For the density of the distribution of the halo we adopt the form of Dasso *et al.* [20]

$$\rho_n = (k/2\pi) \frac{exp(-2kr)}{r^2} \tag{19}$$

where the exponential slope k is adjusted to reproduce the measured value $< r^2_{rms} >^{1/2}$= 2.73 fm of ^{11}Be nucleus [21]. In the same time, k is related to the separation energy S_n=0.504 MeV by the relation

$$(\hbar k)^2 = 2\mu S_n \tag{20}$$

where μ is the effective mass of the core-halo system [4, 18]. When S_n decreases, the tail of the matter distribution becomes longer. From both of the adjustments (using the rms radius or Eq. (20)) we obtain the slope k equals $\sim$ 0.148 fm^{-1}. As seen from Eq.(20), when S_n decreases k becomes smaller and thus the tail of the halo distribution becomes longer.

Another form of the density of the 1n-halo is also taken in a Gaussian form as [22]

$$\rho_n = (a\sqrt{\pi})^{-3} exp(-r^2/a^2) \tag{21}$$

where the a parameter is adjusted to reproduce $< r^2_{rms} >^{1/2}$= 2.73 fm. The ^{208}Pb nuclear matter density is taken in the fermi form as [13]

$$\rho_{^{208}Pb}(r) = \rho_0/[1 + exp(\frac{r - 6.80}{0.515})] \tag{22}$$

The computer code HIOPTM-94 [23] is used to carry out elastic scattering calculations. For the sake of confirmation elastic scattering calculations are repeated using DWEIKO code [24]. Both codes result in identical outputs.

3 Results and discussion

The resulted nuclear matter density of ^{11}Be nucleus (16) using the halo density defined by versions D1 (19) and D2 (21) are shown in Fig.(1) in comparison with that of the ^{10}Be core nucleus (17). It is clear that at r< 5 fm the density of ^{11}Be is mainly formed from the core. However, at r> 5 fm the contribution from the halo is superior. When we adjusted the k parameter in the density of the halo to $< r^2_{rms} >^{1/2}$= 2.93 fm [25] a negligible effect is noticed.

Both versions of the halo density defined by, Eqs.(19) and (21) , yield an extended tail in the ^{11}Be density. However, all over the surface region (3-8 fm) , the density using D1 version

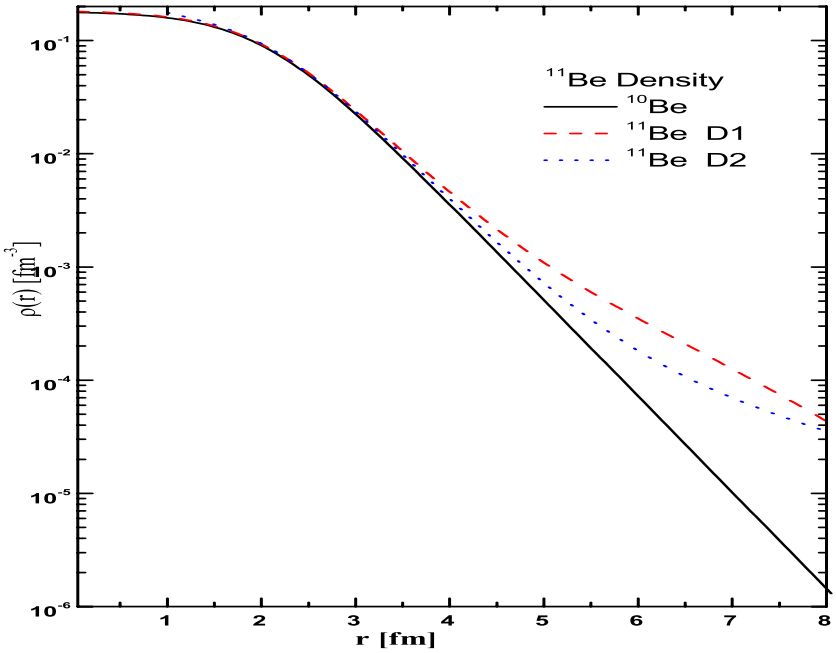

Figure 1: Nuclear matter density distributions of ^{11}Be.

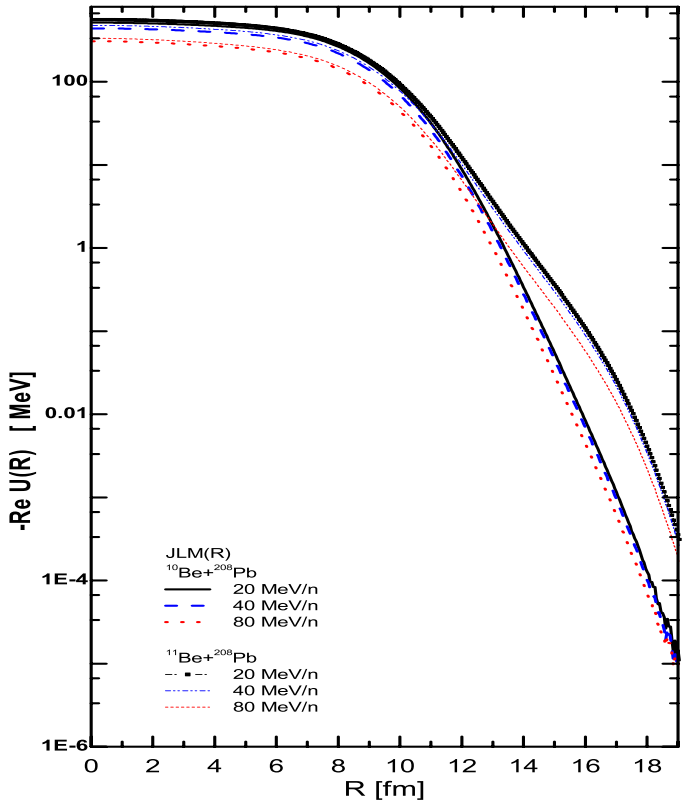

Figure 2: The real part of the optical potentials generated based upon the JLMR effective interactions obtained from expression (5).

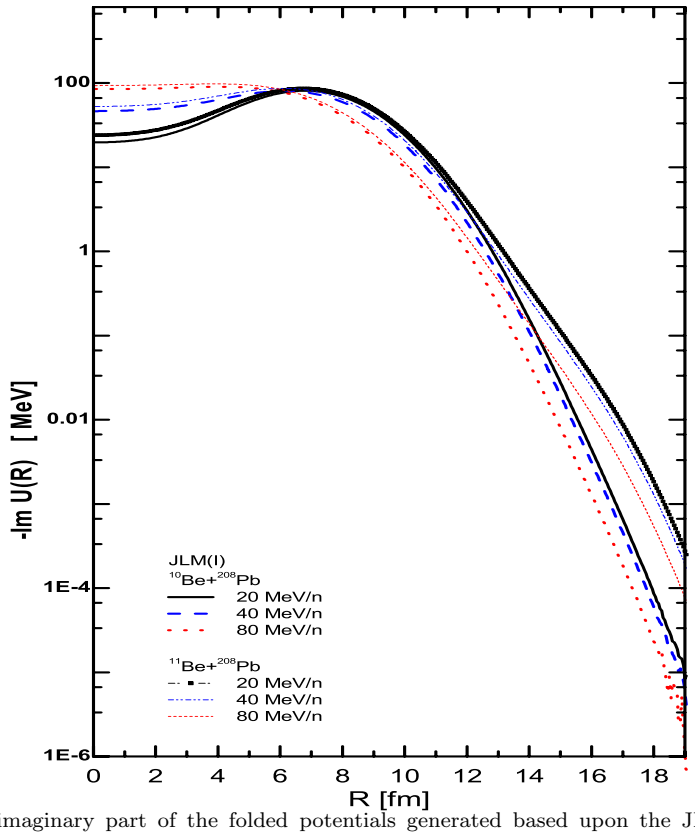

Figure 3: The imaginary part of the folded potentials generated based upon the JLMI effective interactions obtained from expression (6).

is relatively greater than that using D2 one, although both versions reproduce the same value of the rms , 2.73 fm. The DF real and imaginary potentials are calculated using the two versions of the halo density D1 and D2. However, it is found that , both versions reproduce identical results all over the radial ranges R<8 fm. Therefore, we confined the elastic scattering calculations with D1 versions only. Figure (2) demonstrates the ^{10,11}Be-^{208}Pb real DF potentials based upon the JLM effective interaction at energies of 20, 40 and 80 MeV. It is obvious that, for both ^{10,11}Be potentials the depth decreases with increasing energy all over the shown radial range. In the mean time, we notice that, at all considered energies, both potentials coincide in the inner region (R< 12 fm). However, ^{11}Be potentials are characterized by an extended tail in the surface region. This resembles the behavior of the nuclear matter density illustrated in Fig.1. In Fig.(3) the resulted DF imaginary potentials are shown. A different behavior is noticed in the inner region (R< 6 fm) where the depth of potentials increases as energy increases. In the surface region the behavior is similar to that of real potentials. The angular distributions of the ^{10,11}Be+^{208}Pb elastic scattering differential cross section extracted using the derived density-independent and density-dependent (β_R =β_I =3 fm^2) complex DF potentials are shown in Fig.**??**. It is clear that the density dependence treatment slightly shift the phase of the structure of the angular distribution. Of course, without comparing the calculated cross sections with the corresponding measured ones one can not judge how far the density dependence effect may improve the fits with data or not. On the other hand, we illustrate in Fig.(4) a comparison between the calculated ^{11}Be+^{208}Pb imaginary DF potentials before and

after introducing the DPP composed of the nuclear and Coulomb and surface parts represented, respectively, by Eqs. 12 and 13. It is evident that the DPP is almost negligible in the interior part, R < 13 fm. One may observe also that in the surface part the DF potential is completely neglected with respect to the DPP one, where for instance at R= 20 fm, the latter dominates by a factor of about 103. In the mean time, it is interesting to notice that superiority of the Coulomb part with respect to the nuclear one dominates as R increases; at 20 fm the Coulomb part is 10 times the nuclear one while at 30 fm this factor grows up to 100. This is clearly a reflection of the long range effects of the Coulomb potential itself and of the core-recoil it causes[16]. Figure7 shows the calculated cross section at 20 MeV/nucleon. It is evident that the DPP clearly reduces the derived values in the angular range $\Theta_{CM} \geq 7$. It is obvious also that the Coulomb breakup reduces the elastic scattering more than the nuclear breakup. Regarding the angular distributions extracted at 40 and 80 MeV/nucleon, as shown respectively, in Figs. (6 and 7) , one may notice that as energy increases the effect of the breakup potential quantitatively and qualitatively increases.

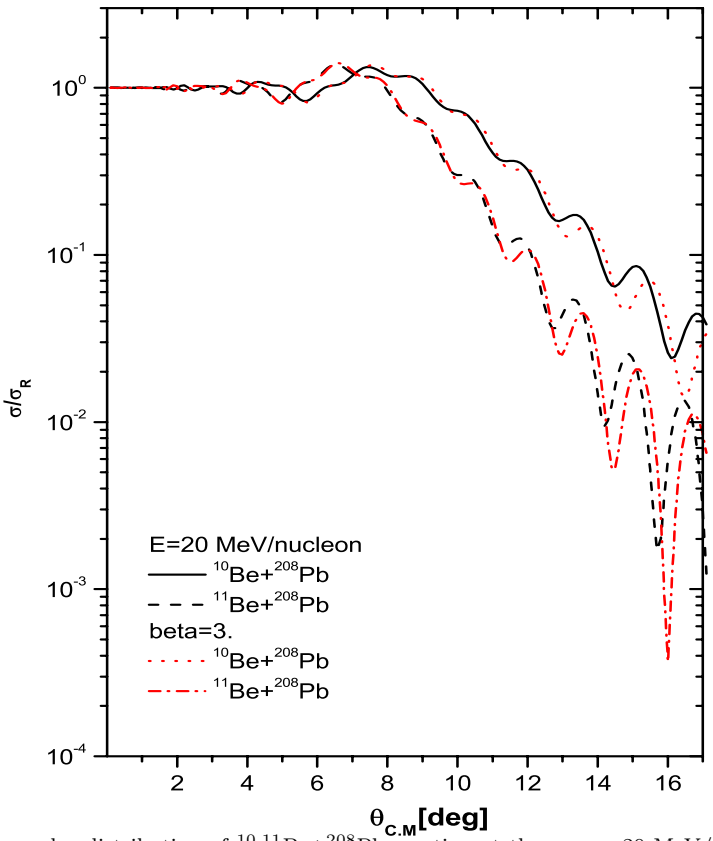

Figure 4: The angular distribution of ^{10,11}Be+^{208}Pb reaction at the energy 20 MeV/nucleon with and without the density dependence of the JLM interaction.

The anomaly of ^{11}Be projectile with the DF potential based upon the JLM interaction is noticed where a reducing renormalization factor (B_R=3) is required . This behavior is attributed to the break-up effect of the loosely bound nucleus ^{11}Be. Therefore, we investigate, the effect of involving the dependence on the projectile and target densities in the effective NN interaction by using the density-dependent version of the JLM interaction.

We tested the effect of an imaginary parts $W_S^N(r, E)$ and $W_S^C(r, E)$ of the DPP on the results. It

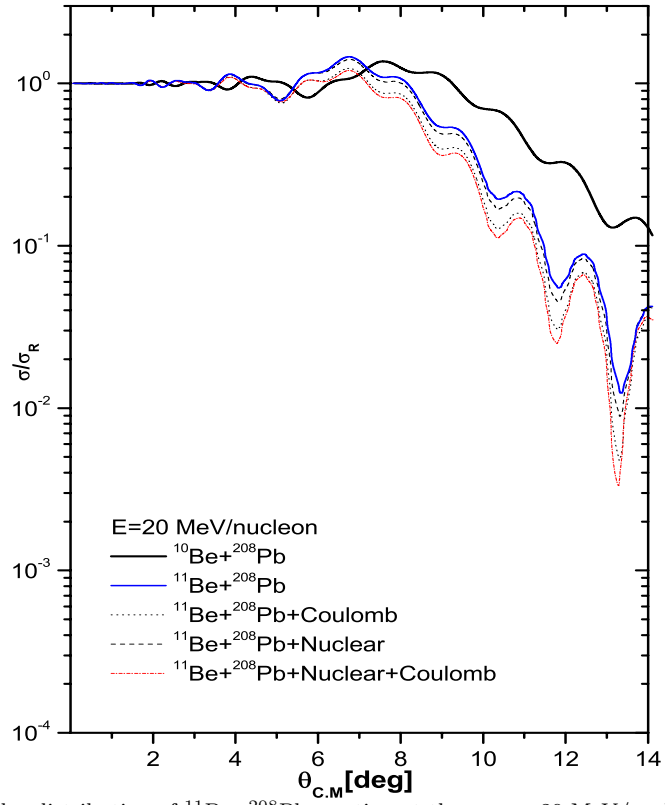

Figure 5: The angular distribution of ^{11}Be+^{208}Pb reaction at the energy 20 MeV/nucleon with and without the breakup effects(Coulomb , Nuclear and Coulomb+Nuclear breakup)

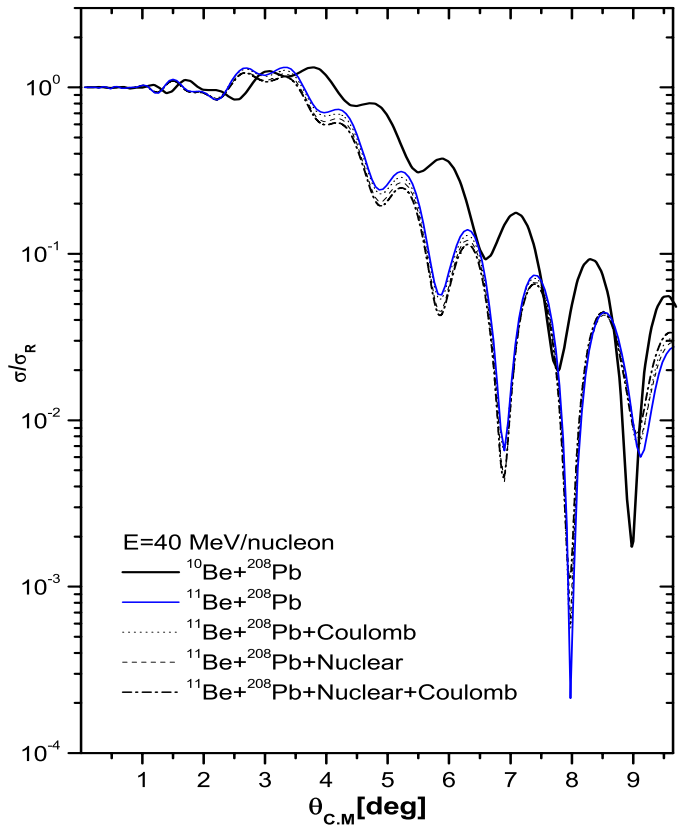

Figure 6: Same as Fig (5) but for 40 MeV/nucleon

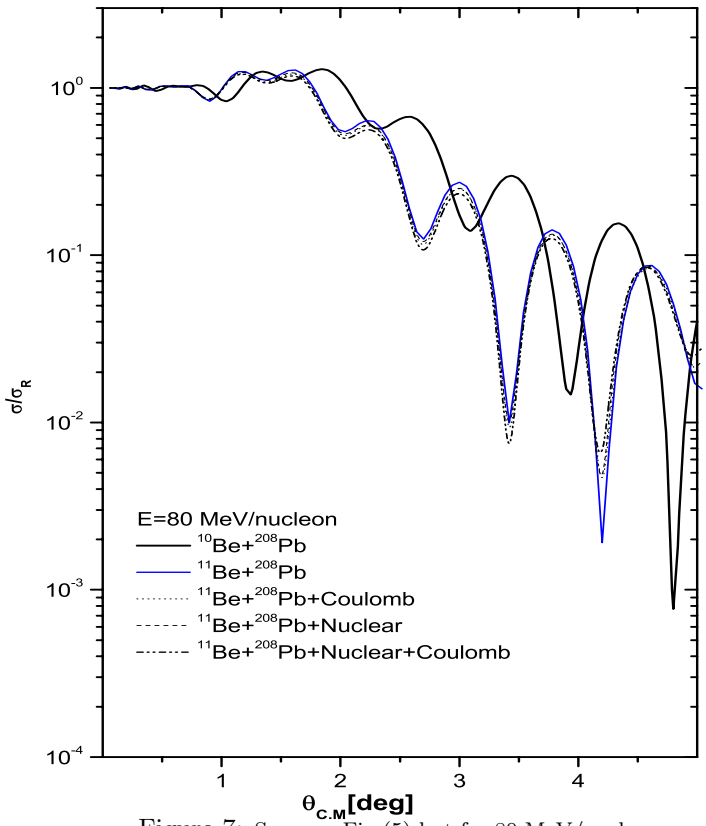

Figure 7: Same as Fig (5) but for 80 MeV/nucleon

was found, however, that involving an imaginary DPP which improve the ability of the DF potential to reproduce the total reaction cross sections data without need to reducing renormalization factor as shown in Table 2., i.e is able to cease the anomaly of ^{11}Be nucleus.

3.1 Total reaction cross section

In the case of a halo projectile, the nucleus-nucleus S-matrix can be written as

$$|S_{NN}|^2 = |S_{CT}|^2 e^{-P_{b_{up}}} \tag{23}$$

where S_{CT} takes into account all core-target interactions while the term $e^{-P_{b_{up}}}$ depends only on the halo neutron breakup probability. For a halo nucleus at high incident energy the transfer probability is going to be much smaller than the breakup probability, therefore the surface potential has been identified here with the breakup potential.

As discussed already in [10], the relation between the total reaction cross section and the breakup cross section, can be understood by expanding the exponential in Eq.(23) to first order in $P_{b_{up}}$ and integrating over the impact parameter b_c. One immediately finds

$$\begin{aligned} 1 - |S_{NN}(b_c)|^2 &\approx 1 - |S_{CT}(b_c)|^2 e^{-P_{b_{up}}(b_c)} \\ &= 1 - |S_{CT}(b_c)|^2 + |S_{CT}(b_c)|^2 (p^N_{b_{up}}(b_c) + p^C_{b_{up}}(b_c)) \end{aligned} \tag{24}$$

Table 1: Optical potential parameters obtained using the real and imaginary JLM folded potentials to analyze the elastic scattering of ^{11}Be+^{208}Pb at 20-80 MeV/nucleon. Real and imaginary volume integrals in MeV.fm^3 are J_R and J_I, total reaction cross section in mb is σ_R ,root mean square radius of real and imaginary potential in (fm) are $\langle r_V\rangle^{1/2}$,$\langle r_I\rangle^{1/2}$,strong absorbtion radius and partial wave are $R_{1/2}$ and $L_{1/2}$.

	E/nucleon	J_R (MeV.fm^3)	$\langle r_V\rangle^{1/2}$ (fm)	J_I (MeV.fm^3)	$\langle r_I\rangle^{1/2}$ fm	σ_R (mb)	Ł$_{1/2}$	$R_{1/2}$ fm
$^{10}Be+^{208}Pb$	20	337.0	7.33	101.3	7.04	3782	192	10.6
$^{11}Be+^{208}Pb$	20	336.3	7.42	101.3	7.13	4021	214	10.8
$^{10}Be+^{208}Pb$	40	513.1	7.37	122.2	7.71	4231	145	11.67
$^{11}Be+^{208}Pb$	40	510.7	7.46	121.9	7.79	4542	162	12.0
$^{10}Be+^{208}Pb$	80	616.4	7.38	130.1	8.07	4163	102	12.3
$^{11}Be+^{208}Pb$	80	613.7	7.48	129.7	8.14	4571	115	12.6
$\underline{\beta_R=\beta_I=3}$								
$^{10}Be+^{208}Pb$	20	163.0	7.50	48.83	7.21	3492	180	10.0
$^{11}Be+^{208}Pb$	20	168.8	7.65	50.68	7.36	3754	204	10.3
$^{10}Be+^{208}Pb$	40	247.6	7.54	58.84	7.85	4019	140	11.3
$^{11}Be+^{208}Pb$	40	256.3	7.69	61.00	7.98	4061	150	11.6
$^{10}Be+^{208}Pb$	80	297.5	7.55	62.36	8.20	4017	100	12.1
$^{11}Be+^{208}Pb$	80	307.9	7.7	64.88	8.32	4264	113	12.4

Table 2: Total reaction cross section in (mb) of ^{11}Be+^{208}Pb at 20-80 MeV/nucleon with and without the DPP effects.

E/nucleon	σ_R (mb)	σ_R^N (mb)	σ_R^C (mb)	σ_R^{tot} (mb)
20	3754	4740	8120	8473
40	4261	4691	6743	7113
80	4264	4177	5285	5634

$$\sigma_{NN} = 2\pi \int b_c db_c \left(1 - |S_{NN}(b_c)|^2\right) \quad (25)$$

$$\approx \sigma_{CT} + \sigma^N_{b_{up}} + \sigma^C_{b_{up}}. \quad (26)$$

The fact that the cross sections values of Table 2. are in very good agreement with the relations contained in Eqs.(25) and (26) is a proof of the accuracy of the hypothesis Eq.(23) for the nucleus-nucleus S-matrix and of the separation of the imaginary potential into a volume and a surface term, with the surface term identified with the halo breakup potential.

4 Conclusions

In the present work, we have used the standard optical model to analyze the differential cross section of ^{11}Be+^{208}Pb elastic scattering at 20-80 MeV/nucleon through the double folding approach supplemented by an analytical form to the dynamic polarization potential (DPP). The double folding model with an energy target density dependent Jeukenne, Lejeune, and Mahaux JLM effective nucleon-nucleon interaction is used to obtain both real and imaginary parts of the central optical potential. The dependence of the potential on densities of projectile and target nuclei in a factorized form is considered. This result is consistent with that obtained recently [8] from the analysis of the same reaction. It would therefore seem that breakup does play an important role in the elastic scattering of ^{11}Be nucleus, and that when properly included it may be possible to describe the scattering without a renormalization of the folded potential. New experiments are needed to measure the cross section at different energies and on different targets in order to systematically study the folded optical potential and find general trends of the breakup reactions.

References

[1] I. Tanihata et al., Phys.Rev. Lett. 55 (1985) 2676; I. Tanihata et al. Phys. Lett B206 (1988) 592.

[2] I. Tanihata, Nucl.Phys. **A488** (1988) 113c.

[3] A. Ozawa et al., Nucl. Phys. A691 (2001) 599; P.G. Hansen, et al., Annu. Rev. Nucl. Sci. 45 (1995) 591; M. Lewitowicz et al., Nucl. Phys. A562 (1993) 301.

[4] I. Tanihata, Proceedings of the Seventh International Conference on Nucleus-Nucleus Collisions, Strasbourg, France, 2000 [Nucl. Phys. A685 (2001)80c]; J. Phys. G22 (1996) 157 and references therein.

[5] F. Cappuzzello et al., Phys. Lett. B516 (2001) 21.

[6] D.T. Khoa, G.R. Satchler and W. vo Ortzen, Phys. Rev. C51 (1995) 2069.

[7] V. Lapoux et al., Phys. Rev. C66 (2002) 034608.

[8] Awad A. Ibraheem and Angela Bonaccorso, Nucl. Phys. A 748 (2005)414.

[9] J. P. Jeukenne, A. Lejeunne and C. Mahaux, *Phys. Rev.* **C16**, 80 (1977).

[10] A. Bonaccorso and F. Carstoiu, Nucl. Phys. A 706 (2002) 322.

[11] A. Bonaccorso, D. M. Brink and L. Lo Monaco, J. Phys. G 13 (1987) 1407.

[12] D. M. Brink, *Semiclassical methods for nucleus-nucleus scattering*, Cambridge University Press. Cambridge. 1985.

[13] M. El-Azab Farid and M. A. Hassanain, *Nucl. Phys.* **A678**, 39 (2000); *ibid*, **A697**, 183 (2002); *Eur. Phys. J.* **A19**, 231 (2004).

[14] J.Cook , Comput. Phys. Commun 25(1982)125.

[15] Awad A. Ibraheem, Modified Version of DFPOT(2007)(unpublished).

[16] Awad A. Ibraheem, *Ph. D.* Thesis, Al-Azhar University, Assiut, Egypt, 2004 (unpublished).

[17] R. Kanungo and C. Samanta, Nucl. Phys. A617 (1997)265 and refernces therein.

[18] A. Bhagwat, Y.K. Gambhir, S.H. Patil, Eur. Phys. J. A8 (2000) 511.

[19] R.E. Warner et al., Phys. Rev. C54 (1996) 1700.

[20] C.H. Dasso, J.L. , S.M. Lenzi and A. Vitturi, Nucl. Phys. A597 (1995) 473.

[21] P. Descouvemont, Nuclear Phys. A699 (2002) 463.

[22] A.K. Chaudhuri, Phys. Rev. C49 (1994) 1603; R.A. Rego, Nucl. Phys. A581 (1995)119.

[23] N.M. Clarke, (1994) (unpublished).

[24] C. A. Bertulani, C. M. Campbell and T. Glasmacher,
Comput. Phys. Commun. 152 (2003) 317 and private communication.

[25] A. Ozawa et al., Nucl. Phys. A693 (2001) 32.